



Damping Properties of a Novel Soft Core and Hard Shell PBA/PMMA Composite Hydrosol Based on Interpenetrating Polymer Networks

Li-Ying Wan^{1,2*}, Le-Ping Chen¹, Xiao-Lin Xie¹, Zhi-Peng Li¹,
and Hong-Qin Fan¹

(1) School of Material Science and Engineering, Nanchang Hangkong University,
Jiangxi Province 330063, P.R. China

(2) State Key Laboratory for Modification of Chemical Fibers and Polymer Materials,
Donghua University, Shanghai 201620, P.R. China

Received 19 November 2010; accepted 6 July 2011

A B S T R A C T

The novel "core - shell" polyacrylate composite hydrosols based on interpenetrating polymer networks (IPN) were synthesized through a new two-step and soap-free emulsion polymerization with seed hydrosol particles with no additional emulsifier. The diameter of the hydrosol particles is much smaller than that of the conventional emulsion, so it makes hydrosol particles show much better stability and coating film properties. The obtained "core-shell" composite hydrosol particles formed by the soft core of BA copolymer and the hard shell of MMA copolymer were characterized by infrared analysis and transmission electron microscope (TEM). The damping properties of polyacrylate IPN, linear IPN, copolymer and blend composed of the same recipe were investigated by dynamic mechanical analysis (DMA) and scanning calorimetry (DSC). The results indicated that the polyacrylate IPN hydrosol exhibited the best damping properties because of its microheterogeneous structure and the synergy effect between both BA and MMA components. While, the polyacrylate copolymer demonstrates only a narrow glass transition range and the polyacrylate blend demonstrates only two independent narrow glass transition ranges. The damping properties of the PBA/PMMA IPN hydrosol were investigated in details through different series of experiments. The results demonstrated that the IPN achieved better damping properties and processing performance under the conditions of 100% neutralization of AA with DEAE, DVB cross-linking agent content of 0.1% and MMA/BA as main monomers with a ratio of 6/4. As far as the novel soft core and hard shell P(BA-co-HEMA)/P(MMA-co-AA-co-HEMA) composite hydrosol is concerned, its damping properties are mainly due to the ratio of main monomers MMA/BA presented in this work.

Key Words:

damping;
IPN;
hydrosol;
core-shell.

INTRODUCTION

Various damping materials have been widely used in missiles, naval vessels, rockets, satellites automobiles and machinery industries. Polymers, as damping materials, play critical role in high-tech fields. If the movement of macromolecular chains cannot keep pace with the outer vibration rate in the glass transition temperature (T_g)

region, the macromolecular chain friction may develop, where, part of the vibration may be absorbed and then dissipated by heat, giving rise to lower vibration amplitude.

In general, the glass transition regions of homopolymers or copolymers are very narrow, thus, the effective damping temperature usually range within 20-30°C in

(*) To whom correspondence to be addressed.
E-mail: wlygood@mail.dhu.edu.cn

the vicinity of T_g [1]. To meet the requirements of practical damping applications, a material should exhibit a high loss factor ($\tan \delta > 0.3$) over a temperature range of about 60-80°C, the damping efficiency is affected not only by the height of the peak, but also by the peak width at the same time [2,3]. However in IPN, two cross-linked network polymers interpenetrate which may exhibit broad glass transition range (ΔT_g) useful in damping purposes and therefore, IPN as a unique microheterogeneous structure can be considered as a new approach for polymer modification [4]. IPN's compatibility is improved at molecular level between the copolymer and blend. Sperling research works indicate that part of polyacrylate IPNs exhibits good damping properties in view of the broad platform region in $\tan \delta - T$ plots and broad ΔT_g in DSC plots [5]. As a result, polyacrylate IPN has attracted considerable attention as damping material [6]. When polyacrylate is used as damping functional material, the maximum value of loss factor $(\tan \delta)_{\max}$ and ΔT_g are the two most important quantities in designing damping materials [7]. However the morphology of a polyacrylate is directly related to its damping properties [8-10].

In this work, PBA/PMMA as an IPN composite hydrosol has been synthesized through "core-shell" two-step and soap-free emulsion polymerization with seed hydrosol particles which are different from the previous seeded emulsion polymerization [11-16]. The soap-free hydrosol does not contain the additional emulsifier and thus the hydrosol, due to its much smaller particle diameter (0.01-0.1 mm) relative to that of the emulsion (0.1 mm), has better stability [17]. Because of the absence of emulsifier in the soap-free hydrosol coating film, the product has better lustre, water resistance, and mechanical properties [18].

The inside and outside parts of the "core-shell" particles are different chemical components [19] and therefore, the fine composite particle demonstrates excellent performance which is almost unachievable by random copolymers or physical blends [20]. Various research groups have studied core-shell structured waterborne coatings composed of a low T_g polymer core and a high T_g polymer shell [21,22]. Although designing core-shell polymethacrylate/polyacrylate systems with latex IPN and the damping

properties of films have been reported earlier, most systems exhibit a narrow damping temperature range.

In a semi-compatible system, like the PBA/PMMA system studied here, the damping properties of polyacrylate IPN, linear IPN, copolymer and the blend have been investigated on the same composition recipe, and the polyacrylate IPN polymer has exhibited the best damping properties. The morphology and damping properties of core-shell structured IPN depend on the synthetic conditions as well as physical parameters such as, relative hydrophobicity of the monomers [23], the mobility of the polymer chains [24], and the chemical or physical interactions between different components [6,25]. As far as the novel soft core-hard shell P(BA-co-HEMA)/P(MMA-co-AA-co-HEMA) composite hydrosols are concerned, their damping properties are mainly due to the main monomeric MMA/BA ratios used in this work.

EXPERIMENTAL

Materials

Methyl methacrylate (MMA), *n*-butyl acrylate (BA), acrylic acid (AA), β -hydroxyethyl methacrylate (HEMA) were purified by reduced pressure distillation before use. Divinylbenzene (DVB) was washed away for removing its inhibitor with NaOH solution 10%. Benzoyl peroxide (BPO) was recrystallized for purification before use as initiator. Isopropanol (IP), ethylene glycol butyl ether (EGBE), *N*-diethylamine ethanol (DEAE), hydrochloric acid were used as received. (All the reagents were purchased from Shanghai Sinopharm Group Co., China)

Synthesis

Synthesis of PBA/PMMA (soft core and hard shell) IPN Composite Hydrosol

P(BA-co-HEMA)/P(MMA-co-AA-co-HEMA) was prepared by a two-step polymerization, that is the preparation of seed hydrosol particles by solution polymerization and then addition of DVB as cross-linking agent in a two-component system. A mixed solvent included 28 mL EGBE and 12 mL IP (volume ratio 7/3) was selected for a reaction mixture of

60 mL MMA, 8 mL AA, 5 mL HEMA and 0.12 mL DVB as the component 1. The whole solution mixture was added drop by drop into a 250 mL four-neck round bottom flask fitted with a PTFE glass stirrer and a reflux condenser to copolymerize for 3 h at 110°C by solution polymerization. It was then cooled to 60°C. A sample of AA was neutralized with DEAE, followed by distilled water added to obtain a 50% solid content hydrosol which was used as seed hydrosol particles. Then, the temperature was raised to 110°C again. Separate volumes of BA (40 mL), HEMA (5 mL) and DVB (0.12 mL) were mixed as component 2 and was added drop by drop to copolymerize on the surface of PMMA seed hydrosol particles for 3 h through soap-free seeded hydrosol polymerization. Then distilled water was added and a 50% solid content composite hydrosol was prepared and subsequently it was cooled down to room temperature.

Synthesis of Linear IPN Hydrosol

Linear IPN was prepared by the same approach as PBA/PMMA IPN, except DVB was absent in the two different component systems.

Synthesis of Copolymer Hydrosol

The total mixed components included 60 mL MMA, 40 mL BA, 8 mL AA, 10 mL HEMA, and 0.24 mL DVB was added drop by drop in a bottle to copolymerize for the hydrosol formation (solid content: 50%).

Synthesis of Blend Hydrosol

Separate volumes of 60 mL MMA, 4 mL AA, 5 mL HEMA and 0.12 mL DVB were mixed as component 1 which was added drop by drop into a round-bottom flask and copolymerized for preparing the hydrosol copolymer 1 (solid content: 50%). The reaction components including 40 mL BA, 4 mL AA, 5 mL HEMA and 0.12 mL DVB were mixed as component 2 to prepare the hydrosol copolymer 2 (solid content: 50%) and finally both hydrosols of copolymer 1 and copolymer 2 were physically blended together.

Characterizations of PBA/PMMA IPN Hydrosol

TEM Analysis

IPN hydrosol was diluted and uniformly dispersed by

ultrasonic treatment, and then the sample was poured dropwise on the surface of copper mesh and dried at room temperature. TEM was carried out with Hitachi H-800 (Japan) transmission electron microscope (TEM) for the observation of particle morphology.

Purification of IPN

The hydrosol was neutralized with diluted hydrochloric acid to precipitate and then hydrosol sediment was filtered and repeatedly washed with distilled water and vacuum dried at 80°C.

FTIR Analysis

FTIR was carried out with a Nicolet Nexus-670 (USA) instrument by KBr tablet approach.

DMA Analysis

The hydrosol particles were dried at room temperature and compression moulded at 150°C into 60×10×1 mm solid film specimens. DMA Test was carried out with a Rheovibron Model DDV-1 Viscoelastometer (Tokyo Baldwin Co., Japan) under a heating rate of 3°C/min and frequency of 1 Hz.

DSC Analysis

DSC Test was carried out with a Perkin-Elmer DSC (USA) apparatus under a heating rate of 10°C/min during the 2nd heating process.

RESULTS AND DISCUSSION

Monomer Selection

MMA and BA are the main monomers in IPN systems. MMA with high T_g , as a hard monomer, while BA with low T_g , as a soft monomer, were used to tailor the T_g of IPN system. In order to obtain the stable soap-free composite hydrosol, the functional monomers were added. The monomer AA provides carboxyl groups as emulsifier around the surface of component 1 copolymer, where -COOH groups changed to -COO⁻ anions when carboxyl groups were neutralized with DEAE. The hydrosol system was stable due to the contribution of electric and steric repulsions between the -COO⁻ anions of seed hydrosol particles. Another functional monomer was HEMA, which acted as polar monomer

and it was added to the both components of 1 and 2. It enhanced the compatibility and formed an interface between the two components, and meanwhile the stability of hydrosol was further increased because of

the presence of hydrophilic hydroxyl groups.

Different model hydrosols and IPN composite hydrosols were prepared under conditions as indicated in Tables 1-4.

Table 1. Polymers for IPN, linear IPN, the copolymer and the blend.

Sample codes	Recipe
PBA /PMMA IPN (recorded as IPN)	Resin: component 1: MMA (60 mL) + AA (8 mL) + HEMA (5 mL) + DVB (0.12 mL), component 2: BA (40 mL) + HEMA (5 mL) + DVB (0.12 mL) Neutralization degree to AA with DEAE : 100%, BPO: 0.6 g, Solid content: 50%
Linear IPN	the same as IPN, but DVB was not added
The copolymer	MMA (60 mL), BA (40 mL), AA (8 mL), HEMA (10 mL), and DVB (0.24 mL), all monomers as a total mixed component
The blend	MMA copolymer hydrosol (MMA (60 mL), AA (4 mL), HEMA (5 mL), and DVB (0.12 mL)) and BA copolymer hydrosol (BA (40 mL), AA (4 mL), HEMA (5 mL) and DVB (0.12 mL)) are physically blended

Table 2. PBA/PMMA IPN composite hydrosols with different neutralization degrees.

Sample codes	Recipe
N85	85% neutralization degree to AA with DEAE, DVB: 0.12 mL; the others are the same as IPN
N100	100% neutralization degree to AA with DEAE, DVB: 0.12 mL; the others are the same as IPN

Table 3. PBA/PMMA IPN composite hydrosols with different cross-linked densities.

Sample codes	Recipe
C: C0.00	the same as IPN, but DVB content is 0 mL
D: C0.05	the same as IPN, but DVB content is 0.06 mL
E: C0.10	the same as IPN
F: C0.15	the same as IPN, but DVB content is 0.18 mL
G: C0.20	the same as IPN, but DVB content is 0.24 mL

Table 4. PBA/PMMA IPN composite hydrosols at different MMA/BA ratios.

Sample codes	Recipe
H: MMA/BA = 3/7	Resin: 30 mL MMA /70 mL BA, the others are the same as IPN
I: MMA/BA = 4/6	Resin: 40 mL MMA /60 mL BA, the others are the same as IPN
J: MMA/BA = 5/5	Resin: 50 mL MMA /50 mL BA, the others are the same as IPN
K: MMA/BA = 6/4	the same as IPN
L: MMA/BA = 7/3	Resin: 70 mL MMA /30 mL BA, the others are the same as IPN

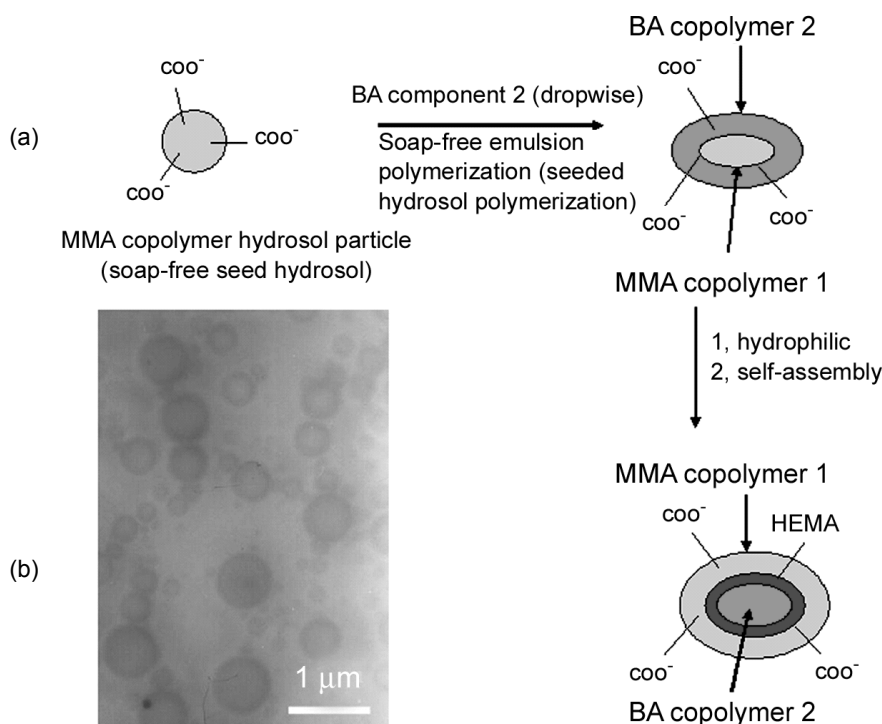


Figure 1. (a) The synthesis route and (b) TEM micrograph of PBA/PMMA (soft core and hard shell) IPN composite hydrosol particles.

Synthesis of PBA/PMMA IPN Composite Hydrosol

The synthetic scheme of PBA/PMMA (soft core and hard shell) IPN is shown in Figure 1a. The component 1 of copolymer including MMA, HEMA, DVB and hydrophilic AA is acted as seed hydrosol via the first step solution polymerization. The component 2 including BA, DVB and HEMA was copolymerized by soap-free emulsion polymerization around the seed hydrosol particles. As a result, the "core-shell" structural composite hydrosol was formed by a two-step polymerization.

In seeded hydrosol polymerization process, the core-shell morphology results from a mechanism involving diffusion of the monomers 2 or its oligomer radicals generated in the aqueous phase into the seed hydrosol particles followed by further propagation step. Subsequently, the seed hydrosol migrates outward after a two-step polymerization because of its strong hydrophilicity and therefore, the MMA hard macromolecular chains move outside and form the shell section. However, BA soft macromolecular chains may penetrate inward because of their

hydrophobic nature and form the core sections. Obviously, two cross-linked components are interpenetrated each other because of different degrees of hydrophilicity leading to an IPN formation. The mutual interpenetrating process enhances the compatibility between MMA and BA components, and finally the stable "core-shell" composite hydrosol particles are self-assembled to form the core of BA copolymer and the shell of MMA copolymer, "core-shell" composite particles have been characterized by TEM, as shown in Figure 1b.

FTIR Analysis of Polyacrylate Copolymer, Blend, and Resulting IPN

The polyacrylate copolymer, blend, and final IPN samples are purified for FTIR after precipitation, the three infrared spectra are very similar, as shown in Figure 2 and Table 5.

There is a strong broad absorption peak in $3600 - 3400 \text{ cm}^{-1}$ which may be attributed to hydrogen bonds between the carboxyl groups of AA and the hydroxyl groups of HEMA. Peaks at 2959 cm^{-1} and 2875 cm^{-1} are the C-H covalent bond vibration bands

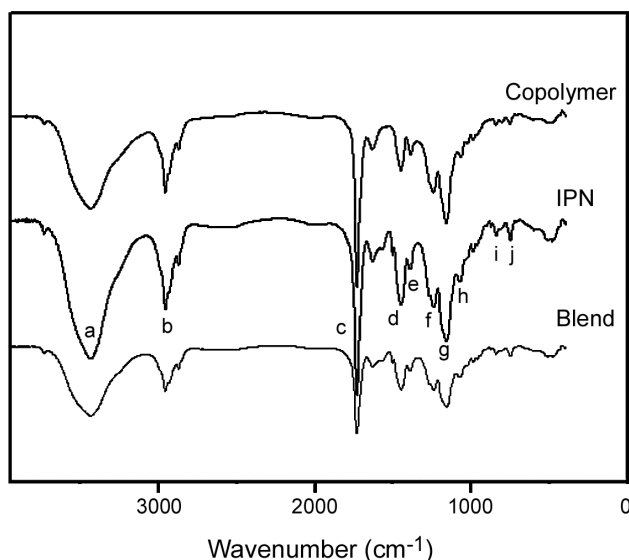


Figure 2. The FTIR Spectra of polyacrylate copolymer, blend, and IPN.

of the main chain of MMA, BA and HEMA. The peak at 1728 cm^{-1} is the C=O carbonyl group stretching vibration band of MMA, BA and HEMA. The peaks at 1454 cm^{-1} and 1391 cm^{-1} are the symmetric stretching vibration characteristic absorption bands of -C-C-O-C of MMA. Similarly, peaks at 1025 cm^{-1} , 990 cm^{-1} and 962 cm^{-1} are the characteristic peaks of BA and those at 842 cm^{-1} and 751 cm^{-1} are the characteristic peaks of DVB. These results indicate that all the monomers have participated in the polymerization reaction.

DMA Analysis of Polyacrylate Copolymer, Blend, IPN and Linear IPN

In order to distinguish the qualities in damping

properties of copolymer, blend, IPN and linear IPN of polyacrylate, we assumed damping materials exhibit good damping ability when $\tan \delta \geq 0.25$. The DMA results are shown in Figures 3a and 3b and Table 6.

Polyacrylate copolymer only demonstrates one loss factor peak but along with a shoulder, the efficient damping range may be broadened slightly due to the semi-compatible characteristics of the multi-component copolymer. Polyacrylate blend demonstrates two independent loss factor peaks, separated by a valley between the BA peak and MMA peak, which means that blending is limited to enhancement of the compatibility between the two components. The BA soft phase and MMA hard phase are still in phase-separation state and therefore polyacrylate blend cannot be used as a good damping material.

Nevertheless, for IPN and linear IPN, the DMA curves of both show two loss factor peaks, where there are broad platforms between the two peaks. This may be the reason that in this region the value of $\tan \delta$ is more than 0.25; an indication that BA soft chains and MMA hard chains are mutually constrained and entangled. The two cross-linked polymer networks are interpenetrated and termed as "synergy effect" that enhances the compatibility between the two components [5]. Therefore, IPN demonstrates special microheterogeneous morphology which is very important for the polymer damping properties.

Moreover IPN damping ability is slightly better than linear IPNs according to the larger area under $\tan \delta - T$ plot in Figure 3b. Due to the addition of cross-linking agent, network cross-linking density of IPN is more completed and the "synergy effect" is

Table 5. FTIR Analysis of polyacrylate copolymer, blend, and IPN.

Infrared bands (cm^{-1})	Types of group vibration	Assignments of absorption peaks
3444(a)	-OH, -COOH stretch	HEMA, AA
2959(b)	-C-H stretch	MMA, BA and HEMA
1728(c)	C=O stretch	MMA, BA and HEMA
1454(d), 1391 (e)	-C-C-O-C stretch	MMA characteristic absorption peaks
1025(f), 990(g), 962(h)	-C-C-O-C stretch	BA characteristic absorption peaks
800(i), 751(j)	C_6H_5^- stretch	DVB

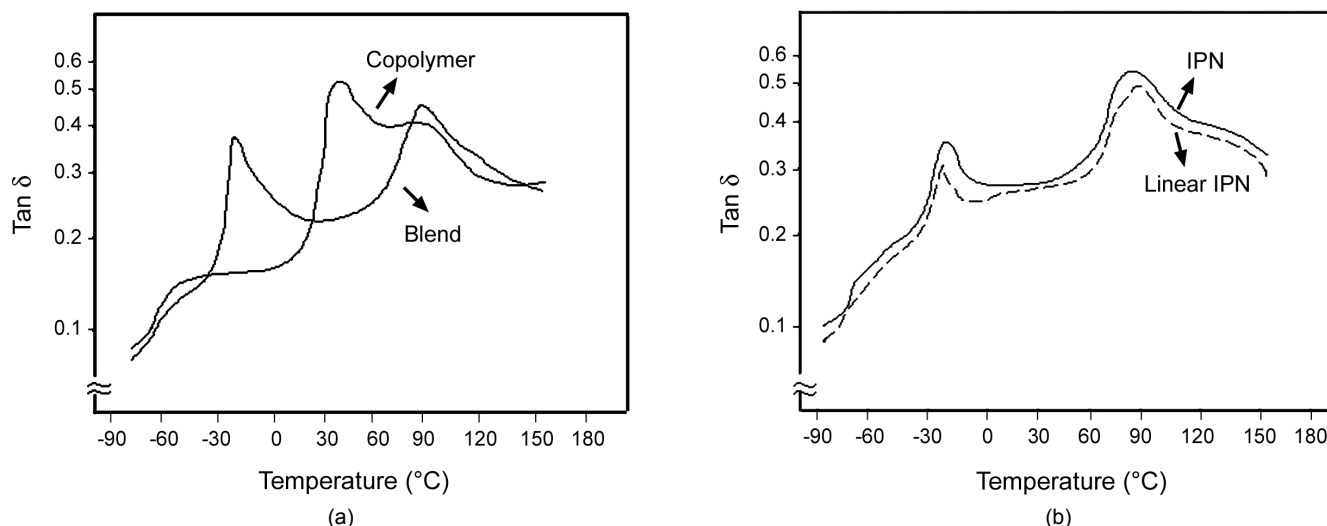


Figure 3. Tan δ vs. T for the copolymer, blend, IPN and linear IPN.

more effective, thus IPN is superior to linear IPN in damping properties.

DSC Analysis of Polyacrylate Copolymer, Blend, IPN and Linear IPN

The ΔT_g is important for damping because there is larger inner friction between the macromolecular chains at this time. The glass transition behaviours of copolymer, blend, IPN and linear IPN are shown in Table 6 and Figure 4.

Copolymer demonstrates one T_g at 42°C, and ΔT_g is narrow of about 40°C. The blend shows two T_g points, one at -20°C for PBA soft phase, which is higher than that of single PBA phase due to its own cross-linking and the influence of PMMA hard phase. Another T_g is at 92.5°C for PMMA hard phase at high temperature. It has slightly shifted to lower

temperature compared to single PMMA phase due to the influence of the PBA soft phase.

However ΔT_g of IPN is about 80°C and ΔT_g of linear IPN is about 70°C, both have only one broad glass transition range that is caused by the interpenetration of the two components. Moreover, ΔT_g of IPN is slightly wider than that of linear IPN, thus IPN is more efficient for damping. The networks of IPN can interpenetrate easier when suitable amount of cross-linking agent is added. On the basis of the above discussion, IPN is superior to copolymer, blend and linear IPN in the design of damping materials.

Effect of Different Factors on IPN Damping Properties

Neutralization Degree of AA with DEAE

The tan δ - T plots of IPNs with different neutraliza-

Table 6. The DMA and DSC data of copolymer, blend, IPN and linear IPN.

Sample	DMA data			DSC data	
	Tan $\delta \geq 0.25$ Temp. range (°C)	(tan δ) _{max}	Peak characteristics	T_g (°C)	ΔT_g (°C)
Copolymer	40-250	0.54	only one peak is about 45°C	42	40
Blend	-30-0, 80-150	0.42	1st peak is about -20°C, 2nd peak is about 92°C	T_{g1} , -18 T_{g2} , 95	38 48
IPN	-34-250	0.55	1st peak is about -20°C, 2nd peak is about 90°C	70	80
Linear IPN	-34-250	0.53	1st peak is about -20°C, 2nd peak is about 90°C	65	70

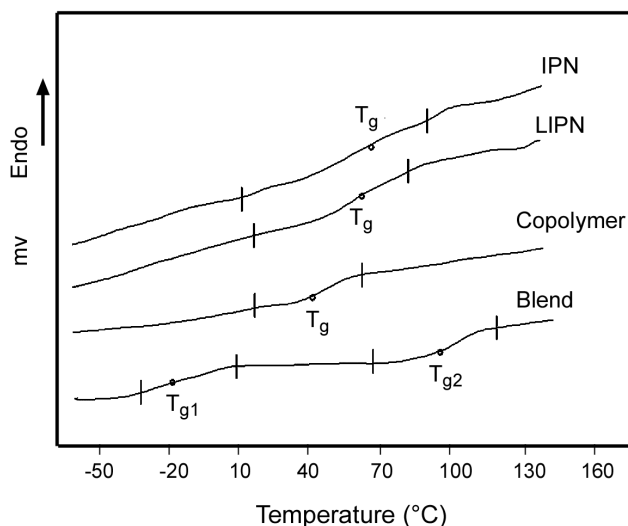


Figure 4. The DSC plots of copolymer, blend, IPN and linear IPN (• represents T_g , and the region between vertical lines represents ΔT_g)

tion degree for 85%, 100% (recorded as N85 and N100, in the order given) are shown in Figure 5. The slight difference indicates that the effect of neutralization degree of AA with DEAE on IPN damping properties is relatively limited.

The $\tan \delta - T$ plots of N85 and N100 both demonstrate two peaks. The first peak for PBA is about -20°C ; the second peak for PMMA is about 95°C . However, the area under $\tan \delta - T$ plot of the N100 is slightly larger than that of N85. The reason is

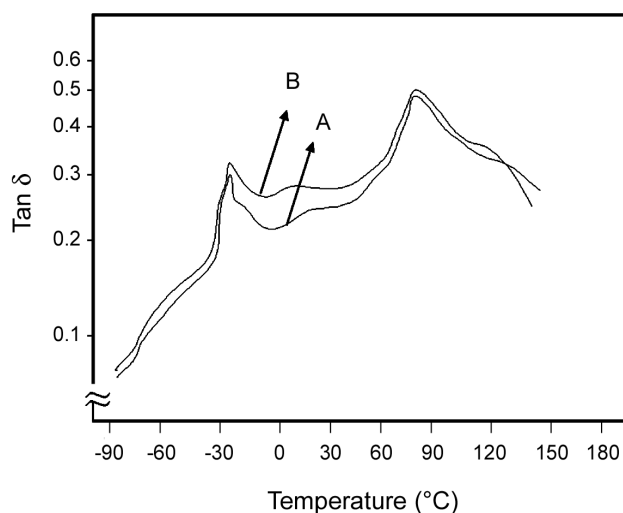


Figure 5. $\tan \delta$ vs. T for different degrees of neutralization (A: N85 and B: N100).

that the polarity of N100 increases with increased $-\text{COO}^-$ content and therefore, the inner friction among macromolecular chains becomes significant.

DVB Concentration as Cross-linking Agent

The amount of DVB as cross-linking agent (volume percentage) under constant MMA/BA ratio of 6/4, was changed as 0.00%, 0.05% (0.06 mL), 0.10% (0.12 mL), 0.15% (0.18 mL), 0.20% (0.24 mL) for their corresponding samples are recorded as C0.00, C0.05, C0.10, C0.15, C0.20, respectively. $\tan \delta - T$ plots of IPNs against DVB amount is shown in Figure 6.

All plots demonstrate two peaks, the first peak for PBA is about -20°C and the second peak for PMMA is about 95°C . Although the DVB amount affects the cross-linked network density, it does not affect the damping properties of PBA/PMMA IPN seriously. First of all, the DVB amount is small and it is only 0.2% of the total volume, secondly, IPN damping properties are mainly determined by the molecular structure of the backbone chain and the side groups which directly contribute to inner friction and energy dissipation. The result is nearly identical to the previous research works [1,26].

In Figure 6, for samples C0.00 to C0.10, the area under the $\tan \delta - T$ plots increases slightly with increase of DVB content, because the cross-linked density of the two networks increases and the

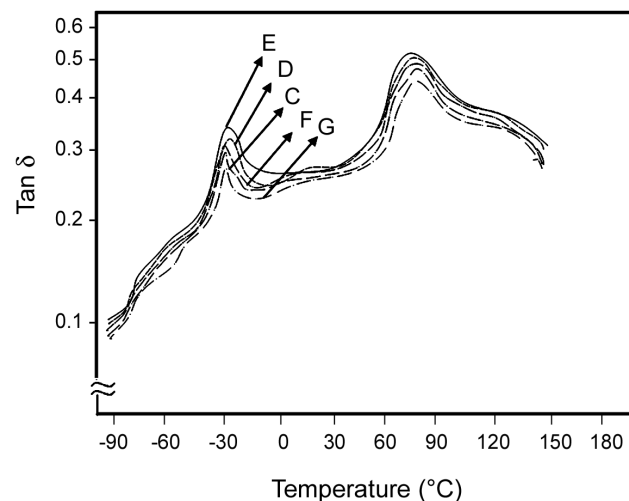


Figure 6. $\tan \delta$ vs. T for different amounts of cross-linking agent (C: C0.00, D: C0.05, E: C0.10, F: C0.15, and G: C0.20).

interpenetration of the networks are more completed, therefore, the damping properties improve slightly.

However, the area under the $\tan \delta - T$ plots is slightly reduced with DVB further increased from sample C0.10 to C0.20. This is due to reduced effective cross-linking density between the components 1 and 2, although the cross-link density of two networks increases. This condition is not suitable for interpenetration of PBA and PMMA two phases, thus synergy effect is weakened. Besides, with the increase in cross-link density, segments of molecules move relatively harder, which lead to reduced damping property. The experiments indicate that 0.10% DVB is the optimum amount for proper damping.

MMA/BA Ratio

As shown in Figure 7, when MMA/BA ratios are in the sequence of 7/3, 6/4, 5/5, 4/6, 3/7, the first peak for PBA is more obvious and the area under the $\tan \delta - T$ plot gradually becomes large with increase of BA content. Because the soft PBA has stronger activities and bigger side groups, its phase may play a more important role on damping. Additionally, soft PBA phase is easy to penetrate into the PMMA hard phase and makes the compatibility improve. Therefore, MMA/BA=3/7 shows the best damping properties.

However, taking IPN processing performance into

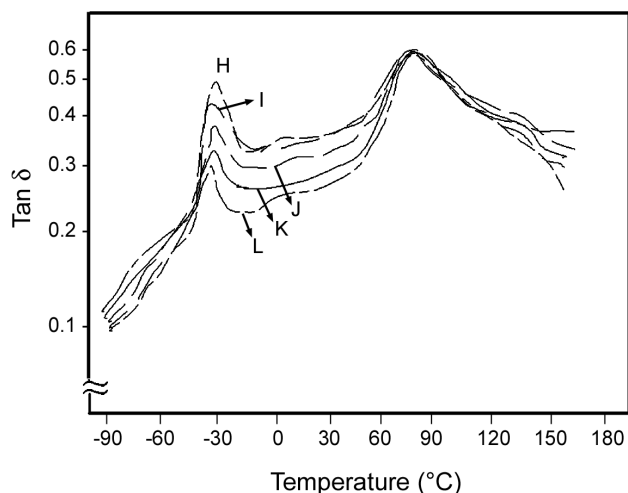


Figure 7. $\tan \delta$ vs. T for different main monomer MMA/BA ratio (H: MMA/BA=3/7, I: MMA/BA=4/6, J: MMA/BA=5/5, K: MMA/BA=6/4, and L: MMA/BA=7/3).

account, e.g., moulding or film forming, PMMA component which acts as a hard shell must be the continuous phase and so it makes IPN display adequate hardness. By comprehensive study on damping properties and processing performance, MMA/BA ratio is obtained to be 6/4.

CONCLUSION

PBA/PMMA (soft core and hard shell) IPN hydrosol has been synthesized through a two-step polymerization with seed hydrosol particles. The $\tan \delta - T$ plots of IPN demonstrate a plateau over a broadened temperature range between the two peaks; the result of synergy effect between the PBA soft phase and PMMA hard phase. The DSC plot of IPN has a broad glass transition range, while copolymer only demonstrates a narrow ΔT_g , the blend demonstrates two independent narrow ΔT_g . The results reveal that the IPN microheterogeneous compatibility plays an important role on damping properties. In order to obtain better damping properties and processing performance, the PBA/PMMA IPN hydrosol is prepared under the conditions of 100% neutralization of AA, 0.1% DVB content and MMA/BA ratio of 6/4.

ACKNOWLEDGMENT

Authors gratefully acknowledge the financial support of Innovation Fund for Ph. D. students of Nanchang Hangkong University (No. EA201001200).

REFERENCES

1. Fradkin DG, Foster JN, Sperling LH, Thomas DA, Molecular demixing in poly[*cross*-(ethyl acrylate)]-inter-poly[*cross*-(methyl methacrylate)] interpenetrating polymer networks brought about by selective decrosslinking and annealing, *Polym Eng Sci*, **26**, 730-735, 1986.
2. Hu R, Dimonie VL, El-Aasser MS, Pearson RA, Hiltner A, Mylonakis SG, Sperling LH, Multicomponent latex IPN materials. I. Morphology control, *J Polym Sci Polym Chem*, **35**,

- 2193-2206, 1997.
- Hu R, Dimonie VL, El-Aasser MS, Pearson RA, Hiltner A, Mylonakis SG, Spearling LH, Multicomponent latex IPN materials: 2. Damping and mechanical behavior, *J Polym Sci Polym Phys*, **35**, 1501-1514, 1997.
 - Klempner D, Frisch KC, *Advances in Interpenetrating Polymer Networks*, Technomic, Lancaster, PA, USA, Vol 2, 18-25, 1990.
 - El-Aasser MS, Hu R, Dimonie VL, Sperling LH, Morphology, design and characterization of IPN-containing structured latex particles for damping applications, *Colloids Surf A*, **153**, 241-253, 1999.
 - Suresh KI, Vishwanatham S, Bartsch E, Viscoelastic and damping characteristics of poly(*n*-butylacrylate)-poly(*n*-butylmethacrylate) semi-IPN latex films, *Polym Adv Technol*, **18**, 364-372, 2007.
 - Mok MM, Kim J, Torkelson JM, Gradient copolymers with broad glass transition temperature regions: design of purely interphase compositions for damping applications, *J Polym Sci Polym Phys*, **46**, 48-58, 2008.
 - Wang YQ, Wang Y, Zhang HF, Zhang LQ, A novel approach to prepare a gradient polymer with a wide damping temperature range by in-situ chemical modification of rubber during vulcanization, *Macromol Rapid Commun*, **27**, 1162-1167, 2006.
 - Chu HH, Lee CM, Huang WG, Damping of vinyl acetate-*n*-butyl acrylate copolymers, *J Appl Polym Sci*, **91**, 1396-1403, 2004.
 - Li F, Larock RC, New soybean oil-styrene-divinylbenzene thermosetting polymers. IV. Good damping properties, *Polym Adv Technol*, **13**, 436-449, 2002.
 - Yu XQ, Gao G, Wang JY, Li F, Tang XY, Damping materials based on polyurethane/polyacrylate IPNs: dynamic mechanical spectroscopy, mechanical properties and multiphase morphology, *Polym Int*, **48**, 805-810, 1999.
 - Guo YK, Wang MY, Zhang HQ, Liu GD, Zhang LQ, Qu XW, The surface modification of nanosilica, preparation of nanosilica/acrylic core-shell composite latex, and its application in toughening PVC matrix, *J Appl Polym Sci*, **107**, 2671-2680, 2008.
 - Wu LY, Wang M, Zhang XX, Chen DB, Zhong AY, Organic montmorillonite modified polyacrylate nanocomposite by emulsion polymerization, *Iran Polym J*, **18**, 703-712, 2009.
 - Kang JS, Yu CL, Zhang FA, Effect of silane modified SiO₂ particles on poly(MMA-HEMA) soap-free emulsion polymerization, *Iran Polym J*, **18**, 927-935, 2009.
 - Bakhshi H, Zohuriaan-Mehr MJ, Bouhendi H, Kabiri K, Emulsion copolymerization of butyl acrylate and glycidyl methacrylate: determination of monomer reactivity ratios, *Iran Polym J*, **19**, 781-789, 2010.
 - Mishra S, Singh J, Choudhary V, Synthesis and characterization of butyl acrylate/methyl methacrylate/glycidyl methacrylate latexes, *J Appl Polym Sci*, **115**, 549-557, 2010.
 - Huang ZH, Xie ZM, Li ZM, Crosslinking reaction of polyacrylate soap-free hydrosol with zirconium chelate, *J Appl Polym Sci*, **92**, 3605-3609, 2004.
 - Huang ZH, Xie ZM, Li ZM, Properties of polyacrylate soap-free hydrosol with zirconium chelate, *J Appl Polym Sci*, **88**, 2858-2860, 2003.
 - Omi S, Kohomoto T, Iso M, Effect of crosslinked core on minimum film formation temperature and morphology of composite microspheres, *Polym Int*, **30**, 499-504, 1993.
 - Dos Santos FD, Fabre P, Drujon X, Meunier G, Leibler L, Films form soft-core/hard-shell hydrophobic latexes: structure and thermomechanical properties, *J Polym Sci Polym Phys*, **38**, 2989-3000, 2000.
 - Hidalgo M, Cavaille JY, Guillot J, Guyot A, Perez J, Vassoille R, Polystyrene (1)/poly (butyl acrylate/amide type functional monomer) (2) two-stage emulsion polymers. Synthesis and thermomechanical properties of latex films, *J Polym Sci Polym Phys*, **33**, 1559-1562, 1995.
 - Suresh KI, Othegraven J, Raju KVS, Bartsch E, Mechanistic studies on particle nucleation in the batch emulsion polymerization of -butyl acrylate containing multifunctional monomers, *Colloid Polym Sci*, **283**, 49-57, 2004.
 - Lee DI, Ishikama T, The formation of inverted core shell latexes, *J Polym Sci Polym Chem Ed*, **21**, 147-154, 1983.
 - Dimonie V, EL-Aasser MS, Klein A, Vanderhoff

- JW, Core-shell emulsion copolymerization of styrene and acrylonitrile on polystyrene seed particles, *J Polym Sci Polym Chem Ed*, **22**, 2197-2215, 1984.
25. Stutman DR, Klein A, EL-Aasser MS, Vanderhoff JW, Mechanism of core/shell emulsion polymerization, *Ind Eng Chem Prod Res Dev*, **24**, 404-412, 1985.
26. Wang JY, Liu RY, Li WH, Li YW, Tang XY, Studies on the damping performance of polystyrene/polyacrylate latex IPN, *Polym Int*, **39**, 101-104, 1996.